



## On the Overturning of Gravity Waves

M. S. Longuet-Higgins

*Proceedings of the Royal Society of London. Series A, Mathematical and Physical Sciences*, Vol. 376, No. 1766. (May 19, 1981), pp. 377-400.

Stable URL:

<http://links.jstor.org/sici?sici=0080-4630%2819810519%29376%3A1766%3C377%3AOTOOGW%3E2.0.CO%3B2-A>

*Proceedings of the Royal Society of London. Series A, Mathematical and Physical Sciences* is currently published by The Royal Society.

---

Your use of the JSTOR archive indicates your acceptance of JSTOR's Terms and Conditions of Use, available at <http://www.jstor.org/about/terms.html>. JSTOR's Terms and Conditions of Use provides, in part, that unless you have obtained prior permission, you may not download an entire issue of a journal or multiple copies of articles, and you may use content in the JSTOR archive only for your personal, non-commercial use.

Please contact the publisher regarding any further use of this work. Publisher contact information may be obtained at <http://www.jstor.org/journals/rsl.html>.

Each copy of any part of a JSTOR transmission must contain the same copyright notice that appears on the screen or printed page of such transmission.

---

The JSTOR Archive is a trusted digital repository providing for long-term preservation and access to leading academic journals and scholarly literature from around the world. The Archive is supported by libraries, scholarly societies, publishers, and foundations. It is an initiative of JSTOR, a not-for-profit organization with a mission to help the scholarly community take advantage of advances in technology. For more information regarding JSTOR, please contact [support@jstor.org](mailto:support@jstor.org).

## On the overturning of gravity waves

BY M. S. LONGUET-HIGGINS, F.R.S.

*Department of Applied Mathematics and Theoretical Physics,  
Silver Street, Cambridge CB3 9EW, and Institute of Oceanographic Sciences,  
Wormley, Surrey GU8 5UB, U.K.*

(Received 30 October 1980)

It is shown that an approximation to the initial stages of overturning in an irrotational gravity wave is given by the potential function

$$\chi = \frac{2}{3}ig^{\frac{1}{2}}z^{\frac{3}{2}} + 2Az^{\frac{1}{2}},$$

where  $g$  denotes acceleration due to gravity,  $z$  is a complex coordinate in the plane of motion, and  $A$  is a linear function of the time  $t$ .

By adding to the above expression a third term, linear in  $z$ , an expression is obtained which can describe the development of sharp corners or cusps in the free surface.

### 1. INTRODUCTION

The sight of the sea surface overturning on itself, as when waves break in deep water or on a sloping beach, is familiar to most mathematicians. Yet surprisingly little progress has been made in finding an analytical description of the free surface profile and of the corresponding field of flow. Recently Longuet-Higgins & Cokelet (1976, 1978) demonstrated a purely numerical method of computation in short time-steps, at each step solving an integral equation. But to comprehend the results of such a computation or to handle them conveniently, the numerical calculation needs to be complemented by some exact or approximate analysis.

A purely local solution describing how the free surface can develop a sharp curvature near the overturning tip of a wave crest was described in a companion paper (Longuet-Higgins 1980*b*). Here we propose to find simple expressions to describe the process whereby the whole body of fluid overturns. We are concerned, however, only with the upper part of the wave, not too far from the wave crest.

It has sometimes been suggested (for example by Price (1971)) that a wave breaks only after attaining the limiting form described by Stokes (1880) in which the crest has a sharp corner of  $120^\circ$  (see figure 1). Thus Price proposed an approximate solution in which the  $120^\circ$  corner-flow was taken as an initial configuration. However, observation suggests that, on the contrary, waves generally break without passing through the Stokes configuration, and that the  $120^\circ$  angle is a very special case, not generally attained. This conclusion is strengthened by the recent demonstration that a limiting wave, with a  $120^\circ$  angle at the crest, actually has less energy than is possessed by lower, symmetric waves with rounded crests (see Longuet-Higgins & Fox 1978). Hence the limiting wave must be very difficult to attain

experimentally, for it cannot be built up by gradual shoaling or by normal pressure applied to the surface without the aid of some dissipative process.

The Stokes 120° corner-flow is nevertheless of considerable interest for our investigation. Thus we shall obtain a tentative representation of the initial stage of overturning simply by adding to the Stokes expression some time-varying term representing a *finite* perturbation of the 120° corner-flow. In our model the flow does not actually pass through the Stokes configuration. Indeed, the extent to which the corner-flow is by-passed is a measure of the total dimensions of the overturning.

In any overturning flow, not only is the surface elevation multivalued but more fundamentally the velocity field (extended analytically beyond the free surface) is a multivalued function of the position coordinate. This is dramatically realized when the tip of a 'plunging' breaker first comes into violent contact with the smooth forward face of the wave. The analytic description of such a multivalued velocity field must involve (at the very least) a branch point in the complex potential. The simplest such branch point is of order  $\frac{1}{2}$ , that is to say it involves a square root.

Now the Stokes corner-flow already involves a branch point of order  $\frac{3}{2}$ . If we assume that the branch-point of order  $\frac{1}{2}$  coincides with that of order  $\frac{3}{2}$  we are led immediately to the simple expression for the velocity potential  $\chi$  which is given in equation (2.5) below. A discussion of the corresponding field of flow is described in § 2. In §§ 3 and 4 we show that the boundary conditions may be satisfied asymptotically at infinity by taking the quantity  $A$  in equation (2.5) to be a linear function of the time  $t$ . Then the solution contains two arbitrary constants which may be chosen (§ 5) so as to obtain the best fit of the boundary conditions over the finite part of the wave. The resulting surface profiles are shown in figures 5*a* and *b*.

In the second half of the paper we show that an improved family of solutions can be derived by adding to the potential function  $\chi$  a term that is linear in  $z$ , representing a uniform upwards velocity. Moreover it is then possible to obtain solutions that develop a sharp-pointed cusp at the tip of the wave, as seen in figure 12.

## 2. DESCRIPTION OF THE FLOW

For simplicity we shall assume the flow to be two-dimensional, incompressible, inviscid and irrotational. In general the velocity potential  $\chi$  is then an analytical function of the complex coordinate  $z = x + iy$  (where  $x$  and  $y$  are rectangular coordinates in the plane of motion), and also of the time  $t$ . It is convenient to take the real axis of  $z$  (i.e. the  $x$ -axis) pointing vertically downwards.

Consider a wave crest that is being propagated horizontally to the right. Let us take a reference frame moving to the right with a uniform velocity equal to the phase-speed (suitably defined). Then the flow at some distance below the wavecrest will appear to be backwards, i.e. to the left.

Figure 1 is a representation of Stokes's corner-flow, in which

$$\chi = \frac{2}{3}ig^{\frac{1}{2}}z^{\frac{3}{2}}, \quad (2.1)$$

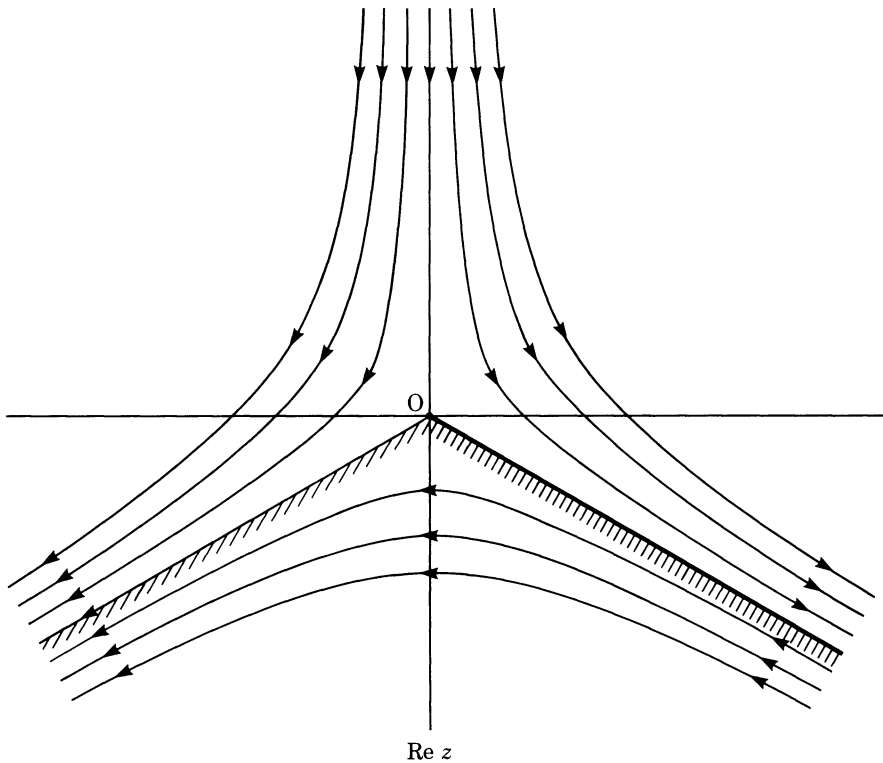


FIGURE 1. Streamlines in Stokes' 120° corner-flow. The fluid occupies the region  $-60^\circ < \theta < 60^\circ$ .

where  $g$  denotes acceleration due to gravity. The free surface consists of the two planes

$$\arg z = \pm \frac{1}{3}\pi. \tag{2.2}$$

The lower streamlines are in the water. The upper streamlines represent an analytic extension of the flow into the 'air' above. Because of the branch-point at  $z = 0$  we have to assume a cut in the  $z$ -plane. In this instance we have taken the cut to lie along the line  $\arg z = \frac{1}{3}\pi$ .

Now in an overturning wave the streamlines are not altogether as in figure 1, but curl back over to the right, as in figure 2. This diagram represents the streamlines of the potential

$$\chi = 2Az^{\frac{1}{2}}, \tag{2.3}$$

where  $A$  is a complex constant:

$$A = -ae^{-i\epsilon}. \tag{2.4}$$

The streamlines are parabolae with foci at  $z = 0$ , and with axes along the line  $\arg z = 2\epsilon$ . In figure 2 we have taken  $\epsilon = 30^\circ$ , so the axes happen to lie along the line  $\arg z = 60^\circ$  which is part of the free surface in figure 1.

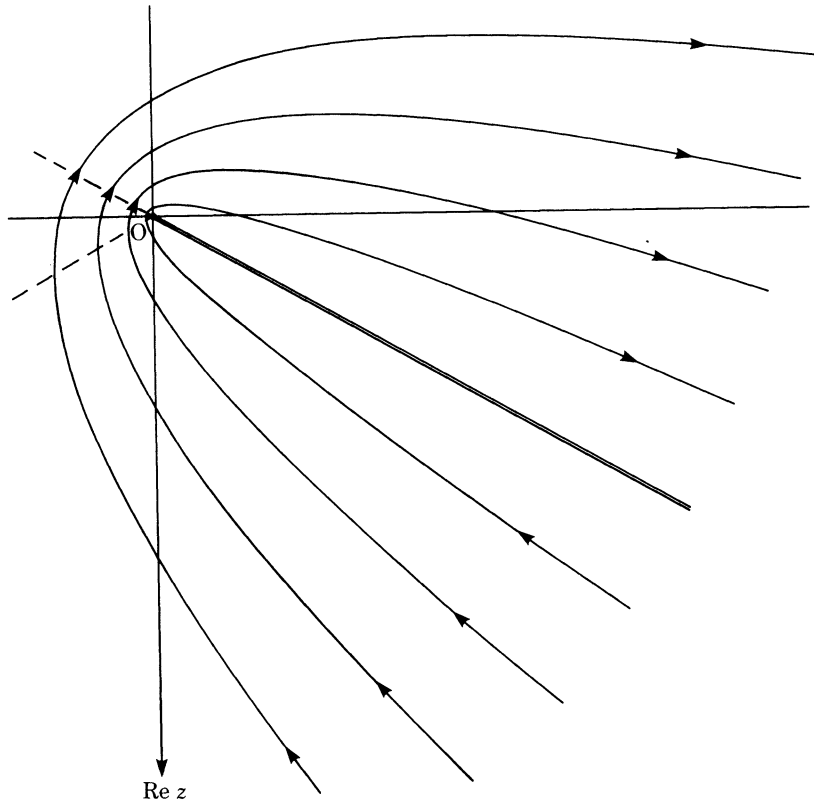


FIGURE 2. Streamlines of the flow  $\chi = e^{\frac{1}{2}i\pi z^{\frac{1}{2}}}$ .

Now let us combine the two flows (2.1) and (2.3) by writing

$$\chi = \frac{2}{3}iz^{\frac{3}{2}} + 2Az^{\frac{1}{2}}. \quad (2.5)$$

(For convenience we choose units in which  $g = 1$ .) The streamlines are shown in figure 3*b*. It will be seen that for large values of  $|z|$  when (2.5) is dominated by the term in  $z^{\frac{3}{2}}$ , the flow is asymptotically like the Stokes corner-flow. On the other hand for small values of  $|z|$ , the term in  $z^{\frac{1}{2}}$  dominates, and the flow resembles the parabolic flow of figure 2.

In general the stagnation point  $z = S$  is given by

$$d\chi/dz = iz^{\frac{1}{2}} + Az^{-\frac{1}{2}} = 0. \quad (2.6)$$

Hence

$$z = iA = -ia e^{-i\epsilon} \quad (2.7)$$

so the vector  $OS$  is inclined at an angle  $\epsilon$  to the horizontal (negative  $y$ -axis).

Another example of the streamlines corresponding to (2.5) is illustrated in figure 3*a*. This corresponds to  $\epsilon = 0$ . We shall show later that it is necessary to add to the expression (2.6) for  $\chi$  a third term representing a uniform upwards flow. Nevertheless it will be useful to discuss first the simpler form (2.6).

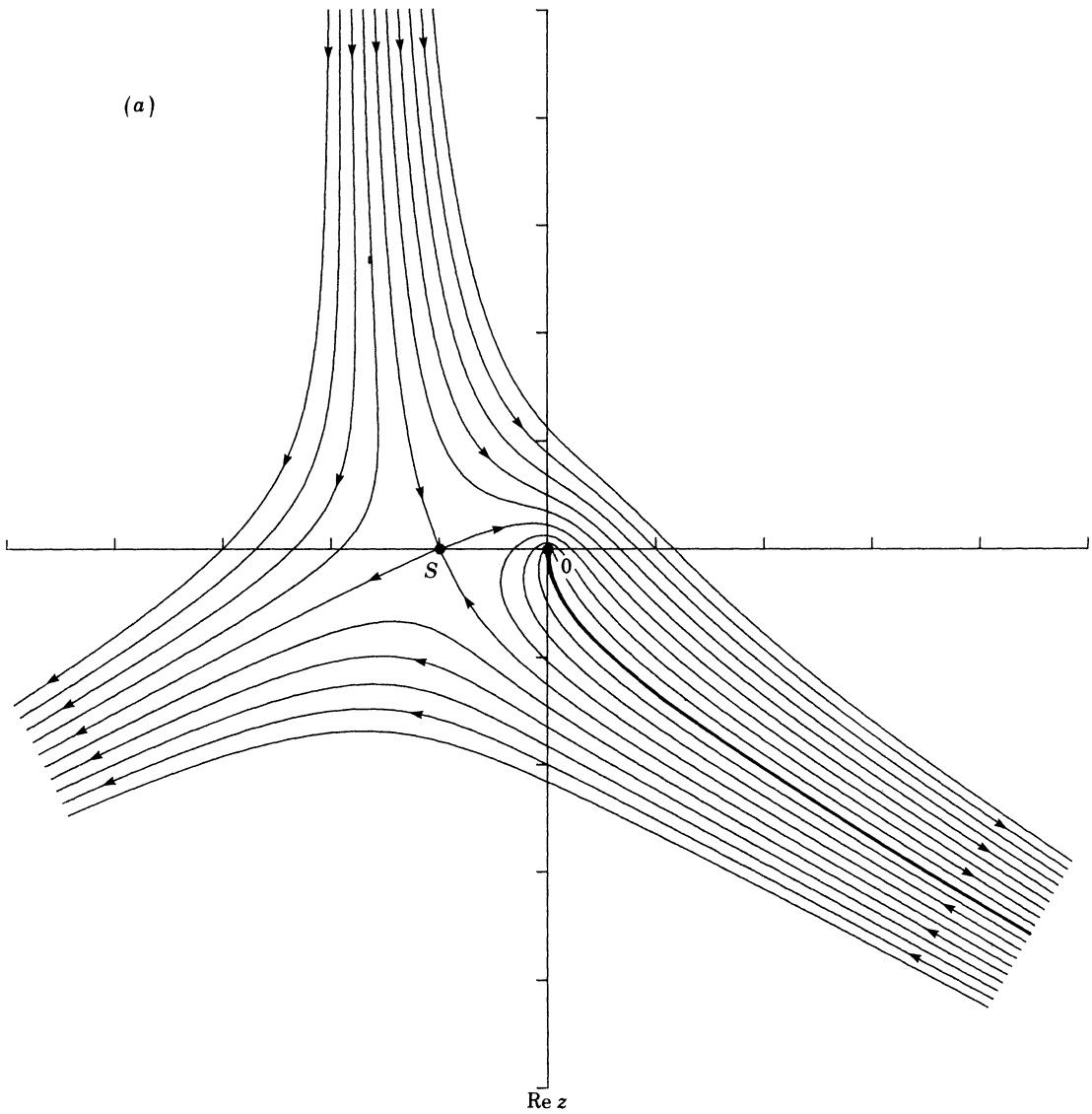


FIGURE 3 (a). Streamlines of the flow given by equation (2.5) when  $\epsilon = 0^\circ$ .

### 3. BOUNDARY CONDITIONS

The flow being time-dependent, the free surface is not in general a streamline, but instead may be specified by the two conditions

$$p = 0, \quad Dp/Dt = 0, \tag{3.1}$$

where  $p$  denotes the pressure and  $D/Dt$  denotes the rate of change following a particle.

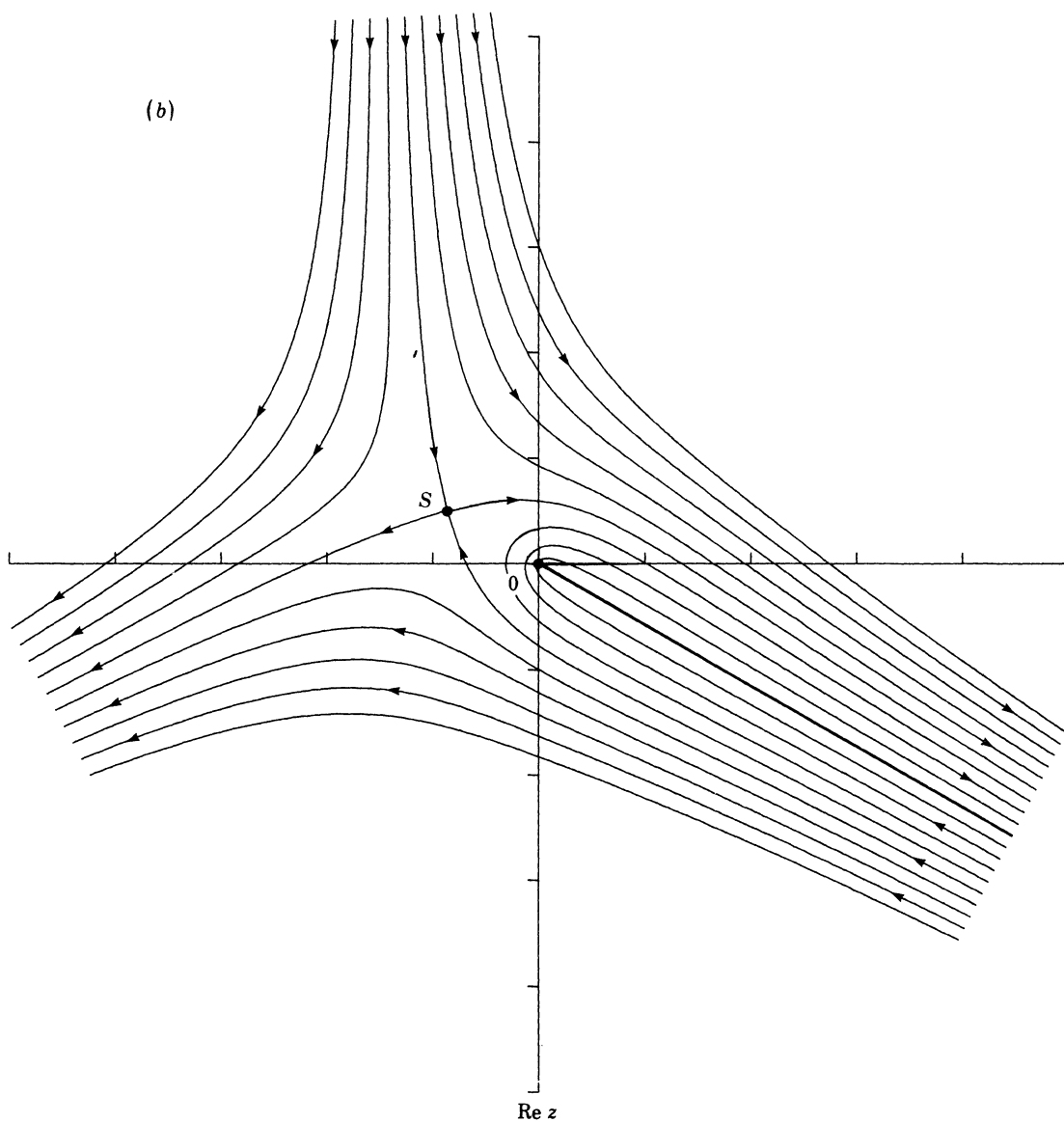


FIGURE 3 (b). Streamlines of the flow given by equation (2.5) when  $\epsilon = 30^\circ$ .

It is convenient to write  $-2p = P$  and  $-2D\rho/Dt = Q$ . General expressions for  $P$  and  $Q$  were derived in Longuet-Higgins (1980a), namely

$$P = \chi_z \chi_z^* + (\chi_t + \chi_t^*) - (z + z^*) - 2F \quad (3.2)$$

and

$$Q = (\chi_z^2 \chi_{zz}^* + 2\chi_z \chi_{zt}^* + \chi_{tt}^*) - \chi_z - \dot{F} + \text{c.c.}, \quad (3.3)$$

where  $F$  is some function of the time  $t$  only, and c.c. denotes the conjugate complex of all preceding terms.

In these expressions let us now substitute

$$\chi = \frac{2}{3}i\omega^3 + 2A\omega, \tag{3.4}$$

where

$$\omega = z^{\frac{1}{2}} \tag{3.5}$$

and  $A$  is a function of the time, to be determined. We have then

$$P = -(\omega^2 - \omega\omega^* + \omega^{*2}) + 2(\dot{A}\omega + \dot{A}^*\omega^*) + i(A^*\omega^2 - A\omega^{*2})/\omega\omega^* - 2F + AA^*/\omega\omega^*, \tag{3.6}$$

the terms being ordered in descending powers of  $|\omega|$ . Also from (3.2)

$$Q = \frac{1}{2}i \frac{\omega^3 - 2\omega^2\omega^* + 2\omega\omega^{*2} - \omega^{*3}}{\omega\omega^*} + 2(\dot{A}\omega + \dot{A}^*\omega^*) + \frac{2i(\dot{A}^*\omega^2 - \dot{A}\omega^{*2})}{\omega\omega^*} - 2\dot{F} + \frac{(A - A^*)(\omega - \omega^*)}{\omega\omega^*} + \frac{A^*\omega^5 + A\omega^{*5}}{2\omega^3\omega^{*3}} + \frac{2(A\dot{A}^* + A^*\dot{A})}{\omega\omega^*} - \frac{iAA^*(\omega^3 - \omega^{*3})}{\omega^3\omega^{*3}} + \frac{i(A^{*2}\omega - A^2\omega^*)}{2\omega^2\omega^{*2}} - \frac{A^2A^*\omega + AA^{*2}\omega^*}{2\omega^3\omega^{*3}}. \tag{3.7}$$

The general problem, as formulated in Longuet-Higgins (1980*a*), is to determine the functions  $A$  and  $F$  so that both  $P$  and  $Q$  shall vanish on the same surface (the free surface). Although this may not be possible over the entire ranges of  $\omega$  and  $t$ , we shall show that over significant ranges of  $\omega$  and  $t$  this can be achieved quite closely.

#### 4. CONDITIONS AS $\omega \rightarrow \infty$

If  $A$  vanished for all  $t$ , then from equations (3.6) and (3.7) we should have

$$Q \equiv \frac{1}{2i} \frac{\omega - \omega^*}{\omega\omega^*} P \tag{4.1}$$

precisely, so that the vanishing of  $P$  implies also the vanishing of  $Q$ . From (3.5) the free surface  $P = 0$  is then given by

$$\omega^2 - \omega\omega^* + \omega^{*2} = 0. \tag{4.2}$$

This represents the pair of straight lines  $\arg(\omega/\omega^*) = \pm \frac{1}{3}\pi$ , that is  $\arg z = \pm \frac{1}{3}\pi$ , as in figure 1.

When  $A$  is not zero, but  $\omega$  is large, we can still ensure that  $Q$  vanishes on the same surface as  $P$  asymptotically, by making

$$Q \equiv \left( \frac{1}{2i} \frac{\omega - \omega^*}{\omega\omega^*} + \frac{\lambda}{\omega\omega^*} \right) P, \tag{4.3}$$

to order 1 as  $\omega \rightarrow \infty$ , where  $\lambda$  is a real constant to be determined. Substituting for  $P$  and  $Q$  from (3.6) and (3.7), and considering only the terms of order  $\omega$  and 1, we see that

$$\dot{A} = 0, \quad (4.4)$$

and

$$2i(\dot{A}^*\omega^2 - \dot{A}\omega^{*2}) - 2\dot{F}\omega\omega^* \equiv -i(\dot{A}\omega + \dot{A}^*\omega^*)(\omega - \omega^*) - \lambda(\omega^2 - \omega\omega^* + \omega^{*2}), \quad (4.5)$$

whence

$$\left. \begin{aligned} 2i\dot{A}^* &= -i\dot{A} - \lambda, \\ -2i\dot{A} &= i\dot{A}^* - \lambda \end{aligned} \right\} \quad (4.6)$$

and

$$-2\dot{F} = i(\dot{A} - \dot{A}^*) + \lambda. \quad (4.7)$$

From (4.6) we have

$$\dot{A} + \dot{A}^* = 0, \quad (4.8)$$

so that  $\dot{A}$  is pure imaginary, and also

$$\lambda = i\dot{A}. \quad (4.9)$$

Then from (4.7)

$$\dot{A} = \frac{2}{3}i\dot{F}. \quad (4.10)$$

Equation (4.4) also implies that

$$\dot{A} = \text{constant}, \quad A = A_0 + \dot{A}t, \quad (4.11)$$

and from (4.10)

$$F = F_0 + \dot{F}t, \quad (4.12)$$

where  $A_0$  and  $F_0$  denote the values of  $A$  and  $F$  when  $t = 0$ . The constants  $A_0$ ,  $F_0$  and  $\dot{F}$  are at our disposal,  $\dot{A}$  being related to  $\dot{F}$  by equation (4.10).

If  $\dot{A} \neq 0$  we may choose the origin of time  $t$  so that  $t = 0$  corresponds to the instant when  $A$  is real. In other words we may choose  $A_0$  to be real. Assuming  $A_0$  to be negative, we may choose units so that

$$A_0 = -1, \quad (g = 1). \quad (4.13)$$

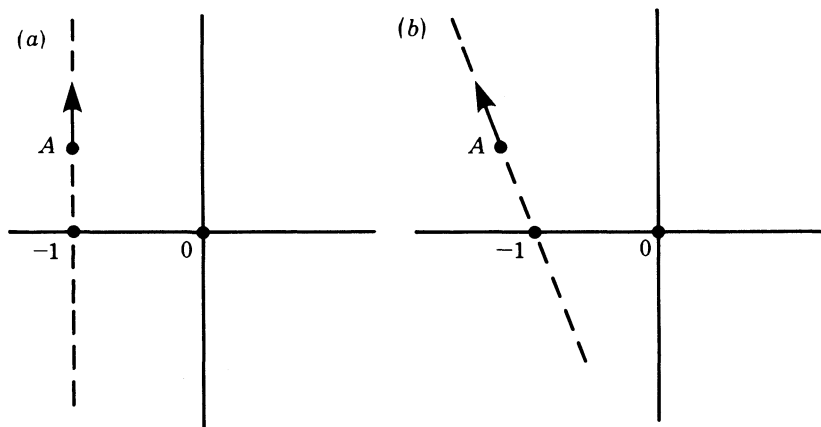


FIGURE 4. Locus of the point  $A(t)$ : (a) when  $U = V = 0$ ;  
(b) when  $U < 0$ ,  $V > 0$ .

as in figure 4. We see then that the expression (2.5), if it is to satisfy the boundary condition as  $\omega \rightarrow \infty$ , has essentially two degrees of freedom, controlled by the two real parameters  $F_0$  and  $\dot{F}$ .

It would be possible to obtain further relations for determining  $F_0$  and  $\dot{F}$  by considering lower-order terms in equation (4.3) but such relations would not necessarily improve the fit of the boundary conditions except at large  $\omega$ . Instead we may choose  $F_0$  and  $\dot{F}$  so as to optimize the fit of the boundary conditions over the *finite* part of the boundary, in the following way.

5. BOUNDARY CONDITIONS FOR FINITE  $\omega$

To determine the two independent parameters  $F_0$  and  $\dot{F}$  we may agree to satisfy the boundary condition  $Dp/Dt = 0$  at a finite number of points (generally not more than two) on the free surface  $p = 0$ . Alternatively, for any given values of  $F_0$  and  $\dot{F}$  we may calculate

$$R(F_0, \dot{F}) = \int \left( \frac{Dp}{Dt} \right)^2 ds \tag{5.1}$$

along the free surface  $p = 0$ , and then adjust  $F_0$  and  $\dot{F}$  so as to make  $R$  a minimum. The latter course has the advantage that the boundary condition is, so to speak, distributed over the range  $-\infty < y < \infty$ , rather than being concentrated at one or two discrete points in the free surface.

Adopting the second method, we find for the values of  $F_0$  and  $\dot{F}$  the following:

$$F_0 = -0.176, \quad \dot{F} = 0.124. \tag{5.2}$$

The corresponding free surface, at  $t = 0$ , is shown in figure 5*a*. A comparison with the streamlines for  $\epsilon = 0$ , which are shown in figure 3*a*, shows that the free surface does indeed intersect the streamlines at a non-zero angle.

To find the form of the free surface at earlier times  $t < 0$  we may proceed backwards, by writing

$$\left. \begin{aligned} F &= F_0 + \dot{F}t, \\ A &= A_0 + \frac{2}{3}i\dot{F}t \end{aligned} \right\} \tag{5.3}$$

and taking  $t = -1, -2, \dots$ , say. (Note that  $\dot{F}$ , not  $F$ , remains constant.) The resulting profiles are shown in figure 5*a* for  $t = 0, -2, -4, \dots, -10$ . As time regresses, the profiles become increasingly rounded. Indeed at  $t = -10$  there is little sign of the overturning to follow, apart from a slight asymmetry in the surface profile.

On the other hand as  $t$  increases from 0 the profiles rapidly become steeper, as shown in figure 5*b*. The profiles are quite similar to those calculated numerically by Longuet-Higgins & Cokelet (1978, figure 21).

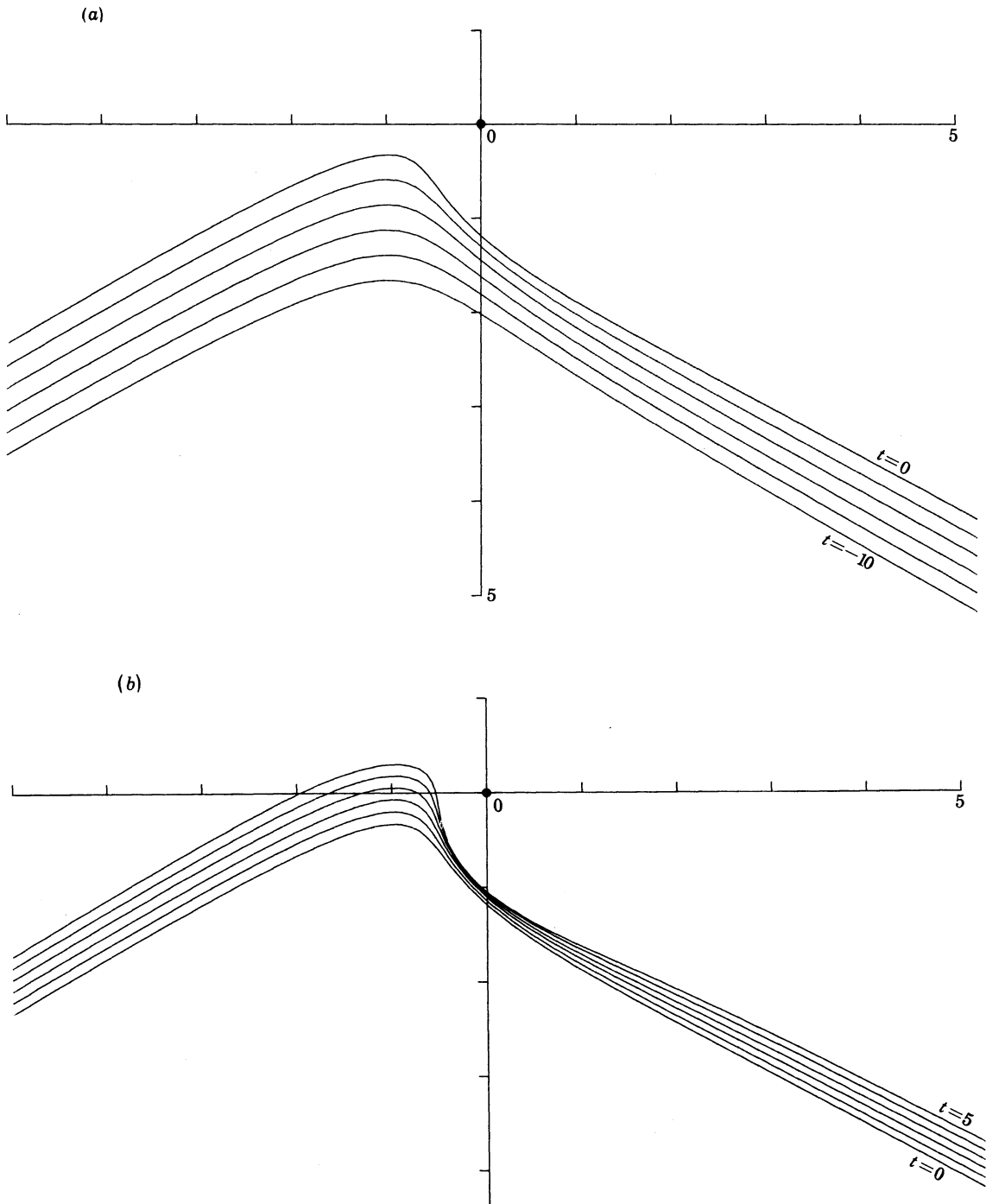


FIGURE 5. The form of the free surface that minimizes  $\int (DP/Dt)^2 ds$  at time  $t = 0$ , for  $U = V = 0$ ,  $A_0 = -1$ ;  $F_0 = -0.176$ ,  $\bar{F} = 0.124$ . (a) Successive profiles of the free surface at previous times:  $t = -10, -8, \dots, 0$ . (b) Successive profiles of the free surface at subsequent times:  $t = 0, 1, \dots, 5$ .

The solution is nevertheless valid only for a limited range of the time  $t$ . In the second half of this paper we shall show that, by adding to (2.5) a further term, linear in  $z$ , it is possible to obtain solutions in which the surface inclination exceeds  $90^\circ$ , and the free surface develops a sharp corner or cusp.

6. A MORE GENERAL MODEL

Now let us adopt the more general expression

$$\chi = \frac{2}{3}i\omega^3 + U\omega^2 + 2A\omega, \tag{6.1}$$

where  $U$  is a constant and  $A = A(t)$  as before. On substituting this expression in equation (3.2) we find

$$\begin{aligned} P = & -(\omega^2 - \omega\omega^* + \omega^{*2}) \\ & + (2A + iU^*)\omega + (2A^* - iU)\omega^* \\ & + i(A^*\omega^2 - A\omega^{*2})/\omega\omega^* + (UU^* - 2F) \\ & + (UA^*\omega + U^*A\omega^* + AA^*)/\omega\omega^*. \end{aligned} \tag{6.2}$$

Likewise if we substitute in equation (3.3) and retain only the terms of highest order in  $|\omega|$  we obtain

$$\begin{aligned} Q = & i(\omega^3 - 2\omega^2\omega^* + 2\omega\omega^{*2} - \omega^{*3})/2\omega\omega^* + 2(\dot{A}\omega + \dot{A}^*\omega^*) \\ & + [(U + 2i\dot{A}^*)\omega^2 - (U + U^* + 2\dot{F})\omega\omega^* + (U^* - 2i\dot{A})\omega^{*2}]/\omega\omega^* \\ & + \dots \end{aligned} \tag{6.3}$$

If we now assume the relation (4.3), then on equating coefficients of the terms of highest order on each side we find

$$\dot{A} = 0 = \dot{A}^* \tag{6.4}$$

as before, but now

$$\left. \begin{aligned} (U + 2i\dot{A}^*) + \lambda - \frac{1}{2}(U^* - 2i\dot{A}) &= 0, \\ (U^* - 2i\dot{A}) + \lambda - \frac{1}{2}(U + 2i\dot{A}^*) &= 0, \\ -(U + U^* + 2\dot{F}) - \lambda + \frac{1}{2}(U^* - 2i\dot{A}) + \frac{1}{2}(U + 2i\dot{A}^*) &= 0. \end{aligned} \right\} \tag{6.5}$$

On eliminating  $\lambda$  from these expressions we have

$$U + 2i\dot{A}^* = U^* - 2i\dot{A}, \tag{6.6}$$

and

$$U + U^* + 2\dot{F} = \frac{2}{3}(U^* - 2i\dot{A}). \tag{6.7}$$

Hence

$$\dot{A} = \frac{2}{3}i(\dot{F} + \frac{1}{2}U - \frac{1}{4}U^*), \tag{6.8}$$

which generalizes equation (4.10).

Let us write

$$U = U + iV, \tag{6.9}$$

where  $U$  and  $V$  are real. Then equation (6.8) becomes

$$\dot{A} = \frac{2}{3}i(\dot{F} + \frac{1}{4}U) - \frac{1}{2}V. \quad (6.10)$$

Conversely

$$\dot{F} = -\frac{1}{4}U - \frac{3}{4}i(\dot{V} + 2\dot{A}). \quad (6.11)$$

The form of the free surface is obtained by writing  $P = 0$  in (6.2). Since from (4.11) and (6.11) we have

$$A = (A_0 - \frac{1}{2}Vt) + \frac{2}{3}i(\dot{F} + \frac{1}{4}U)t \quad (6.12)$$

we obtain

$$\begin{aligned} \omega^2 - \omega\omega^* + \omega^{*2} &= \frac{4}{3}i(\dot{F} + U)(\omega - \omega^*) \\ &\quad + i(A_0 - \frac{1}{2}Vt)(\omega^2 - \omega^{*2})/\omega\omega^* \\ &\quad + \frac{2}{3}i(\dot{F} + \frac{1}{4}U)t(\omega^2 + \omega^{*2})/\omega\omega^* \\ &\quad + (U^2 + V^2 - 2F_0) - 2\dot{F}t \\ &\quad + O(|\omega|^{-1}). \end{aligned} \quad (6.13)$$

Now, introducing polar coordinates by writing

$$z = r e^{i\theta}, \quad \omega = r^{\frac{1}{2}} e^{\frac{1}{2}i\theta}, \quad (6.14)$$

we find, to order  $r^{-1}$ ,

$$\begin{aligned} \cos \theta - \frac{1}{2} &= -\frac{4}{3}(\dot{F} + U)r^{-\frac{1}{2}} \sin \theta \\ &\quad + [\frac{2}{3}(\dot{F} + \frac{1}{4}U) \cos \theta + \frac{1}{2}V \sin \theta - \dot{F}]tr^{-1} \\ &\quad - [A_0 \sin \theta + F_0 - \frac{1}{2}(U^2 + V^2)]r^{-1}. \end{aligned} \quad (6.15)$$

On the forward face of the wave set

$$\theta = \frac{1}{3}\pi + \delta, \quad (6.16)$$

where  $\delta$  is of order  $r^{-\frac{1}{2}}$ . Thus by expanding each side of (6.15) in powers of  $r^{-\frac{1}{2}}$  and by successive approximation we easily obtain

$$\begin{aligned} r\delta &= -\frac{4}{3\sqrt{3}}(\dot{F} + U)r^{\frac{1}{2}} + \frac{4}{3\sqrt{3}}(\dot{F} - \frac{1}{2}U - \frac{\sqrt{3}}{8}V)t \\ &\quad + A_0 + \frac{2}{\sqrt{3}}[F_0 - \frac{1}{2}(U^2 + V^2)]. \end{aligned} \quad (6.17)$$

Similarly on the rear face of the wave if we set  $\theta = -(\frac{1}{3}\pi + \delta)$  we find

$$\begin{aligned} r\delta &= -\frac{4}{3\sqrt{3}}(\dot{F} + U)r^{\frac{1}{2}} + \frac{4}{3\sqrt{3}}(\dot{F} - \frac{1}{2}U - \frac{\sqrt{3}}{8}V)t \\ &\quad - A_0 + \frac{2}{\sqrt{3}}[F_0 - \frac{1}{2}(U^2 + V^2)]. \end{aligned} \quad (6.18)$$

Consider now the implication of these expressions. In (6.17), the quantity  $r\delta$  represents approximately the normal displacement of the free surface above the straight line  $\theta = \frac{1}{3}\pi$ . For large values of  $r$ , the leading term in (6.17) represents a parabola which is concave or convex upwards according to the sign of  $\dot{F} + U$ . For a concave forward face (and convex rear face) we need to have

$$\dot{F} + U < 0. \quad (6.19)$$

The second term on the right of (6.17) or (6.18) represents an upward displacement which is independent of  $r$  but increases linearly with the time. We require that as  $t \rightarrow -\infty$ , so the normal displacement shall be negative, at least when  $r \rightarrow \infty$ . This implies that the coefficient of  $t$  in (6.17) or (6.18) shall be positive, that is

$$\dot{F} - \frac{1}{8}U - \frac{\sqrt{3}}{8}V > 0. \tag{6.20}$$

In the simplest case  $U = V = 0$  discussed in §§ 4 and 5 the two conditions (6.19) and (6.20) are clearly mutually contradictory. In the next-simplest case when  $V = 0$ ,  $U \neq 0$ , the conditions (6.19) and (6.20) imply that

$$U < 8\dot{F} < -8U. \tag{6.21}$$

Hence  $U < 0$ , in other words the imposed uniform velocity must be *upwards*.

A physical interpretation is as follows (see figure 6). On the forward face of the wave the upward uniform velocity combines with the upward component of flow in the Stokes corner-flow (seen in the present frame of reference) to produce a larger value of the absolute velocity, compared with the velocity at an equal distance on the left, where the velocity in the Stokes corner-flow has a downward component. Now from Bernoulli's equation

$$gx = p + \frac{1}{2}q^2 + \phi_t - F, \tag{6.22}$$

it follows that, at two comparable positions 1 and 2 on the right and left respectively,

$$g(x_1 - x_2) = \frac{1}{2}(q_1^2 - q_2^2), \tag{6.23}$$

since at large distances  $\phi_t$  is of order  $r^{-\frac{1}{2}}$  only and so relatively small. The right-hand side of (6.23) is seen to be positive, showing that the displacement of the free surface face is *downwards* on the forward face but upwards on the rear face. The whole wave therefore tends to tilt clockwise.

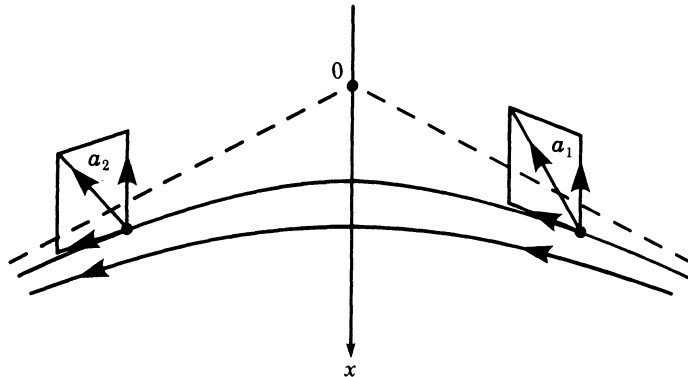


FIGURE 6. A physical interpretation of the role of the upwards vertical velocity ( $U < 0$ ) in equation (6.1).

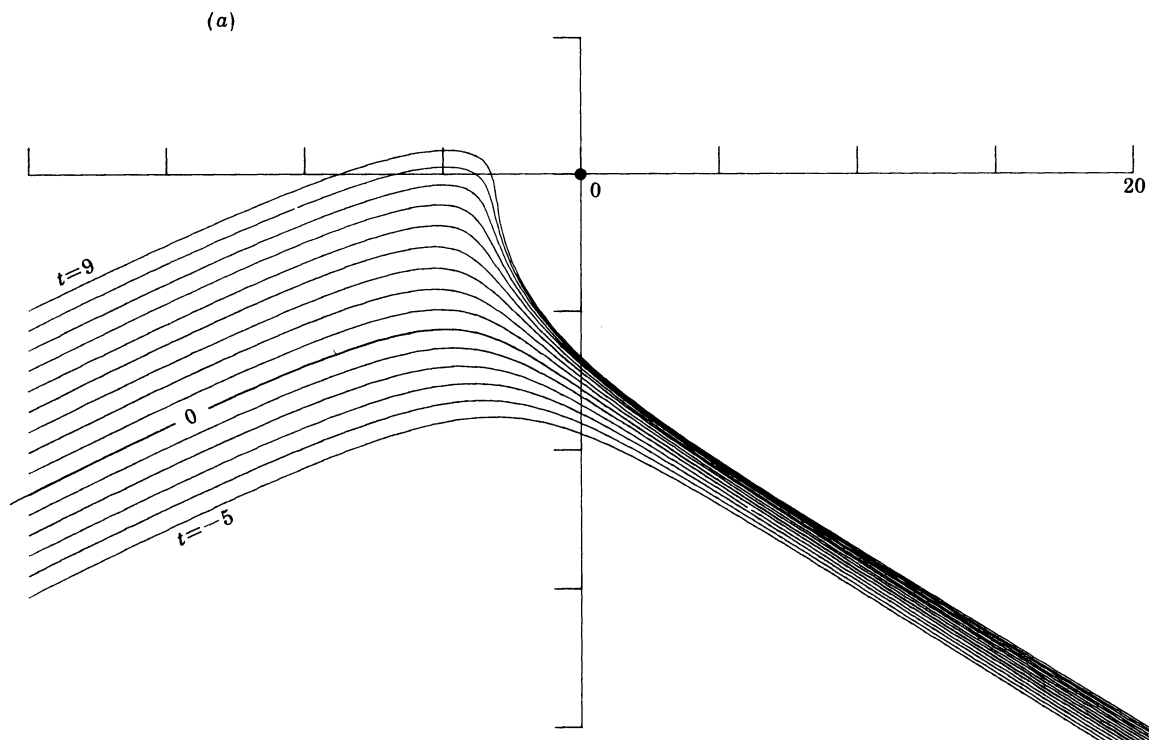


FIGURE 7 (a). Successive positions of the free surface corresponding to equation (6.1) with  $U = -1$ ,  $V = 0.5$ .  $A_0$ ,  $F_0$  and  $\dot{F}$  are chosen so as to minimize  $\int (DP/Dt)^2 ds$  at time  $t = 0$ :  $A_0 = -1.702$ ,  $F_0 = -2.492$ ,  $\dot{F} = 0.403$ .

For given values of  $U$  and  $V$  we may choose the three variables  $A_0$ ,  $F_0$  and  $\dot{F}$  so as to minimize  $\int Q^2 ds$  taken along some central part of the free surface (say  $-10 < Y < 10$ ). In the typical case  $U = -1$ ,  $V = 0.5$  we find the optimum values

$$A_0 = -1.702, \quad F_0 = -2.49, \quad \dot{F} = 0.402.$$

The corresponding r.m.s. value of  $Dp/Dt$  is 0.281.

Successive profiles of the free surface are shown in figure 7. For a quantitative comparison with the profiles calculated numerically by Longuet-Higgins & Cokelet (1978), we may consider the time-history of the maximum surface slope  $\alpha_{\max}$ , shown by the broken curve in figure 8. This suggests that  $d\alpha_{\max}/dt$  reaches a maximum when  $\alpha_{\max}$  is about  $60^\circ$ , or  $t = 6$ . The solid curve in figure 8 corresponds to the profiles from figure 21 of Longuet-Higgins & Cokelet (1978). In these calculations,  $d\alpha_{\max}/dt$  clearly continues to increase steeply beyond  $\alpha_{\max} = 60^\circ$ . Moreover the corresponding time-scales in figure 8 are in the ratio  $\tau \approx 8.8$ . The length-scales, on the other hand, are in the ratio  $l \approx 17.6$ , so that  $\tau/l^{1/2}$  is about 2.1 instead of unity as we might expect ( $g$  is taken as unity in both cases).

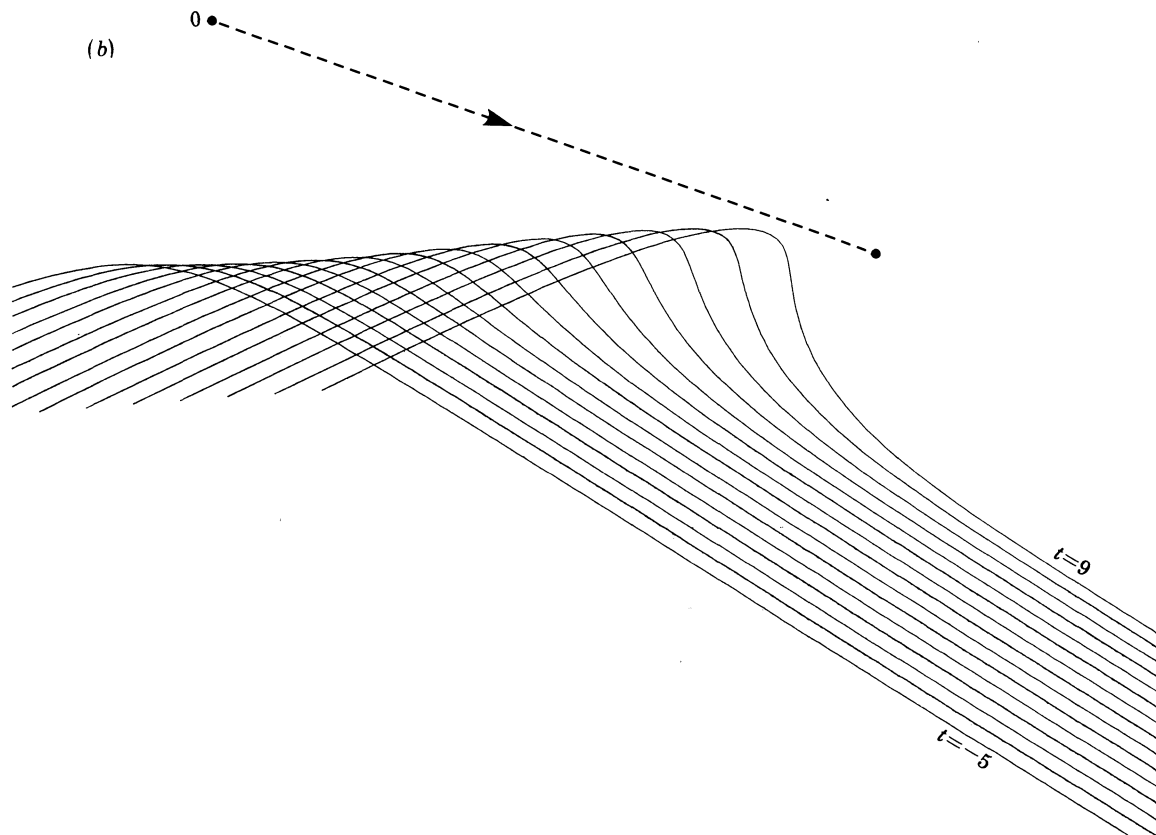


FIGURE 7 (b). As figure 7a, but viewed in a frame of reference travelling with velocity  $(-0.6, -1.7)$ .

The cause of the discrepancy can be traced to the fact that as  $t$  increases  $Dp/Dt$ , instead of remaining small, becomes of order unity near the wave crest. In general the crest appears less sharp-pointed than in observations.

### 7. SHARP CORNERS AT THE FREE SURFACE

In this section we shall enquire whether the form of the velocity potential proposed in equation (6.1) can lead to the formation of a sharp corner at the interface, and possibly even to a cusp.

As shown in Longuet-Higgins (1980a, paper I), the simplest type of sharp corner corresponds to a saddle-point in the pressure field. The general condition for a saddle-point, in terms of the velocity potential  $\chi(z, t)$ , was shown in § 6 of paper I to be

$$\chi_{zz}\chi_z^* + \chi_{zt} = 1 \tag{7.1}$$

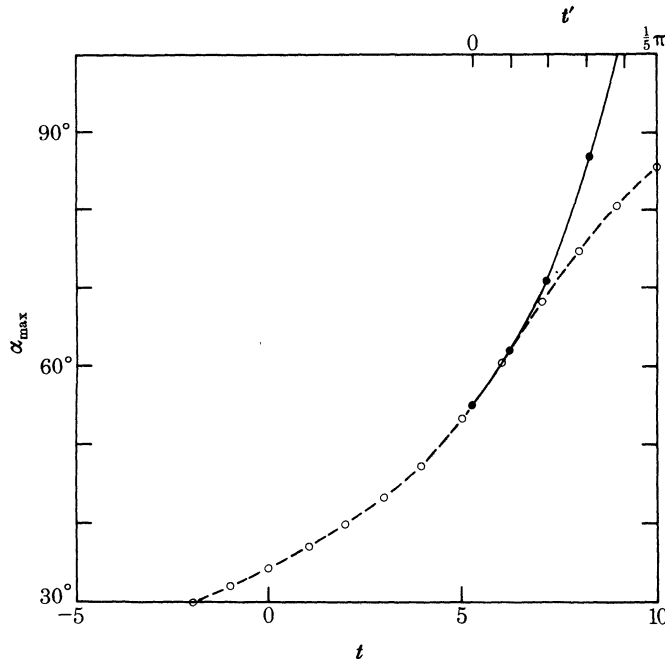


FIGURE 8. The maximum inclination  $\alpha_{\max}$  of the free surface as a function of the time  $t$ .  
 —, From numerical computation (Longuet-Higgins & Cokelet 1978); upper time-scale.  
 - - -, From analytic model (figure 7); lower time-scale.

( $g$  being taken as unity). On substitution for  $\chi$  from (6.1) this gives

$$\frac{1}{2}(i/\omega - A/\omega^3)(-i\omega^* + U^* + A^*/\omega^*) + \dot{A}/\omega = 1, \tag{7.2}$$

where  $\omega = z^{\frac{1}{2}}$  as before. Hence

$$\dot{A} = \omega - \frac{1}{2}\omega^*(1 + iB)(1 + iB^*) + \frac{1}{2}(B - i)U^*, \tag{7.3}$$

where

$$B = A/\omega^2 = A/z. \tag{7.4}$$

Now, if we satisfy the free surface conditions at  $\infty$ , then by § 6

$$\dot{A} + \dot{A}^* = -V. \tag{7.5}$$

On substituting for  $\dot{A}$  from (7.3) and simplifying we obtain

$$(\omega + \omega^*)(1 + BB^*) + [i(\omega - \omega^*) + U](B + B^*) - iV(B - B^*) = 0. \tag{7.6}$$

Then writing  $z = r e^{i\theta}$  as before, so that

$$B = -(a/r)e^{-i(\theta + \epsilon)}, \tag{7.7}$$

we find that equation (7.6) becomes

$$(a/r)^2 - 2\beta(a/r) + 1 = 0, \tag{7.8}$$

where

$$\beta = (-\tan \frac{1}{2}\theta + \frac{1}{2}Ur^{-\frac{1}{2}} \sec \frac{1}{2}\theta) \cos(\theta + \epsilon) - \frac{1}{2}Vr^{-\frac{1}{2}} \sec \frac{1}{2}\theta \sin(\theta + \epsilon). \tag{7.9}$$

Equation (7.8) has two positive real roots

$$a/r = \beta \pm (\beta^2 - 1)^{1/2} \tag{7.10}$$

provided that

$$\beta \geq 1. \tag{7.11}$$

When  $\beta = 1$ , the two roots are coincident. Given  $r$  and  $\theta$  (but not  $a$  or  $\epsilon$ ) a necessary and sufficient condition for (7.11) to be satisfied is that

$$(\tan \frac{1}{2}\theta - Ur^{-1/2} \sec \frac{1}{2}\theta)^2 + (\frac{1}{2}Vr^{-1/2} \sec \frac{1}{2}\theta)^2 \geq 1. \tag{7.12}$$

On writing

$$\left. \begin{aligned} r^{1/2} \cos \frac{1}{2}\theta &= \xi, \\ r^{1/2} \sin \frac{1}{2}\theta &= \eta, \end{aligned} \right\} \tag{7.13}$$

this becomes

$$\xi^2 - (\eta - \frac{1}{2}U)^2 \leq \frac{1}{2}V^2, \tag{7.14}$$

a region whose boundary is a hyperbola in the  $(\xi, \eta)$ -plane. We recover the permissible region in the  $z$ -plane by noting that

$$z = x + iy = (\xi + i\eta)^2 + 2i\xi\eta. \tag{7.15}$$

The region is sketched in figure 9 in the typical case  $V = 0.5$ . When  $V = 0$  the boundary consists of two intersecting parabolas.

To find the angle  $\gamma$  contained between the tangents to the free surface at the sharp corner itself we may make use of the formula

$$\cos \gamma = \chi_{zz}\chi_{zz}^* / |\chi_{zzz}\chi_{zz}^* + \chi_{zzt}|, \tag{7.16}$$

which was proved in Longuet-Higgins (1980*a*). On substituting from equation (6.1) of the present paper and making use of (7.3) we find

$$\cos \gamma = r^{1/2} |1 + iB|^2 / [2 |\omega - BU^* + iB(1 + iB^*)\omega^*|]. \tag{7.17}$$

The condition for a *cusp* is that  $\gamma = 0$  and so

$$\cos \gamma = 1. \tag{7.18}$$

For given values of  $U$  and  $V$ , one further condition may be imposed on the solution. It is natural to specify that  $Dp/Dt = 0$  at the sharp corner itself. Now in general we have

$$Dp/Dt \equiv p_t + \chi_z^* p_z + \chi_z p_z^*. \tag{7.19}$$

At the sharp corner,  $p_z$  also vanishes; hence

$$p_t = 0. \tag{7.20}$$

From the general expression (3.2) for the pressure it follows that we must have

$$\chi_{zt}\chi_z^* + \chi_{tt} - \dot{F} + \text{c.c.} = 0. \tag{7.21}$$

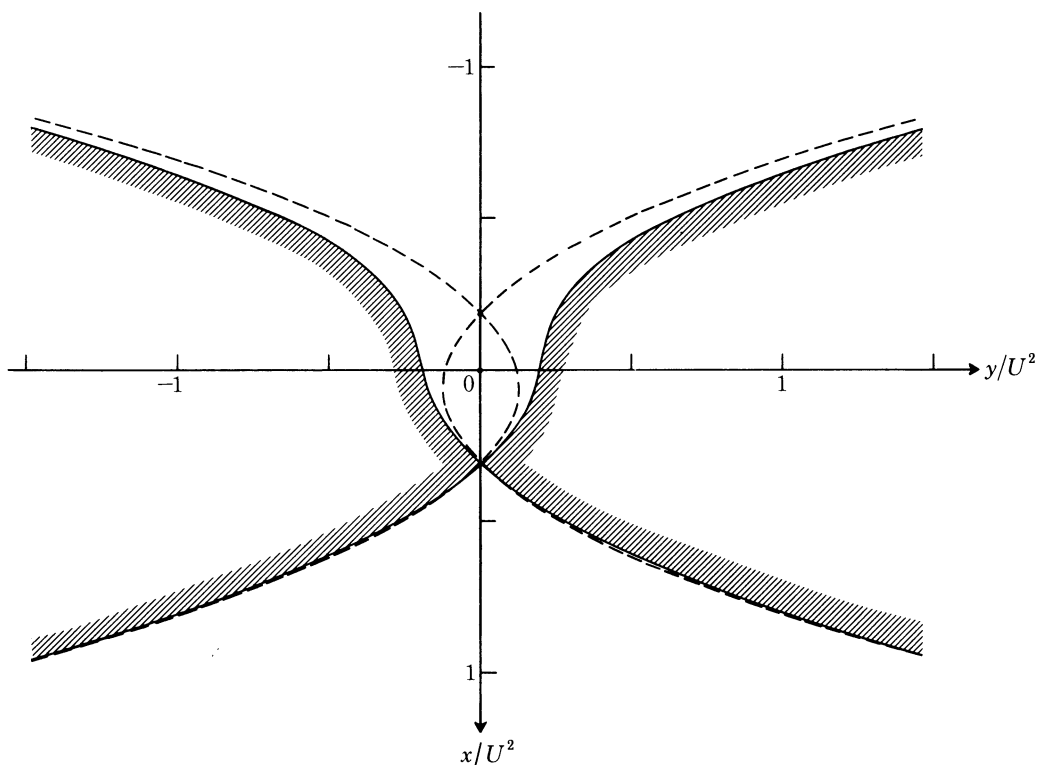


FIGURE 9. Sketch of region in the  $z$ -plane allowing real solutions of equation (7.8). Shaded areas indicate no solution.

Further, since in our model  $\dot{A} = 0$ , we have  $\chi_{tt} \equiv 0$ . Thus (7.21) becomes

$$(\dot{A}/\omega)(-i\omega^* + U^* + A^*/\omega^*) - \dot{F} + \text{c.c.} = 0, \quad (7.22)$$

where  $\dot{F}$  is given in terms of  $\dot{A}$  by equation (6.11).

Altogether, equations (7.10), (7.18) and (7.22) provide three conditions for determining  $a/r$ ,  $\theta$  and  $\epsilon$ , given  $U$  and  $V$ .

To determine the nature of the solution it is convenient to start with the case when  $U = V = 0$  (see the appendix) or equivalently when  $r \rightarrow \infty$  but  $r/a$  remains finite. Then the boundary (7.14) of the permissible zone of solutions to the first condition collapses onto the (horizontal)  $y$ -axis. Solutions may occupy the upper half-plane  $x < 0$ , but differ radically in the left-hand and right-hand quadrants (see figure 10). Solutions with values of  $\gamma$  less than  $60^\circ$ , including the cusps, for which  $\gamma = 0$ , are confined to the left-hand quadrant ( $-180^\circ > \theta > -90^\circ$ ). On the right the only corner-angles are much blunter. The loci corresponding to equation (7.22) reduce to two arcs, shown by dotted lines in figure 10. The cusp-locus  $\gamma = 0$  intersects these in two points, each a possible position of a sharp crest.

To obtain solutions for finite values of  $r = r_c$  it is convenient to take units so that

$$U = -1, \quad g = 1 \quad (7.23)$$

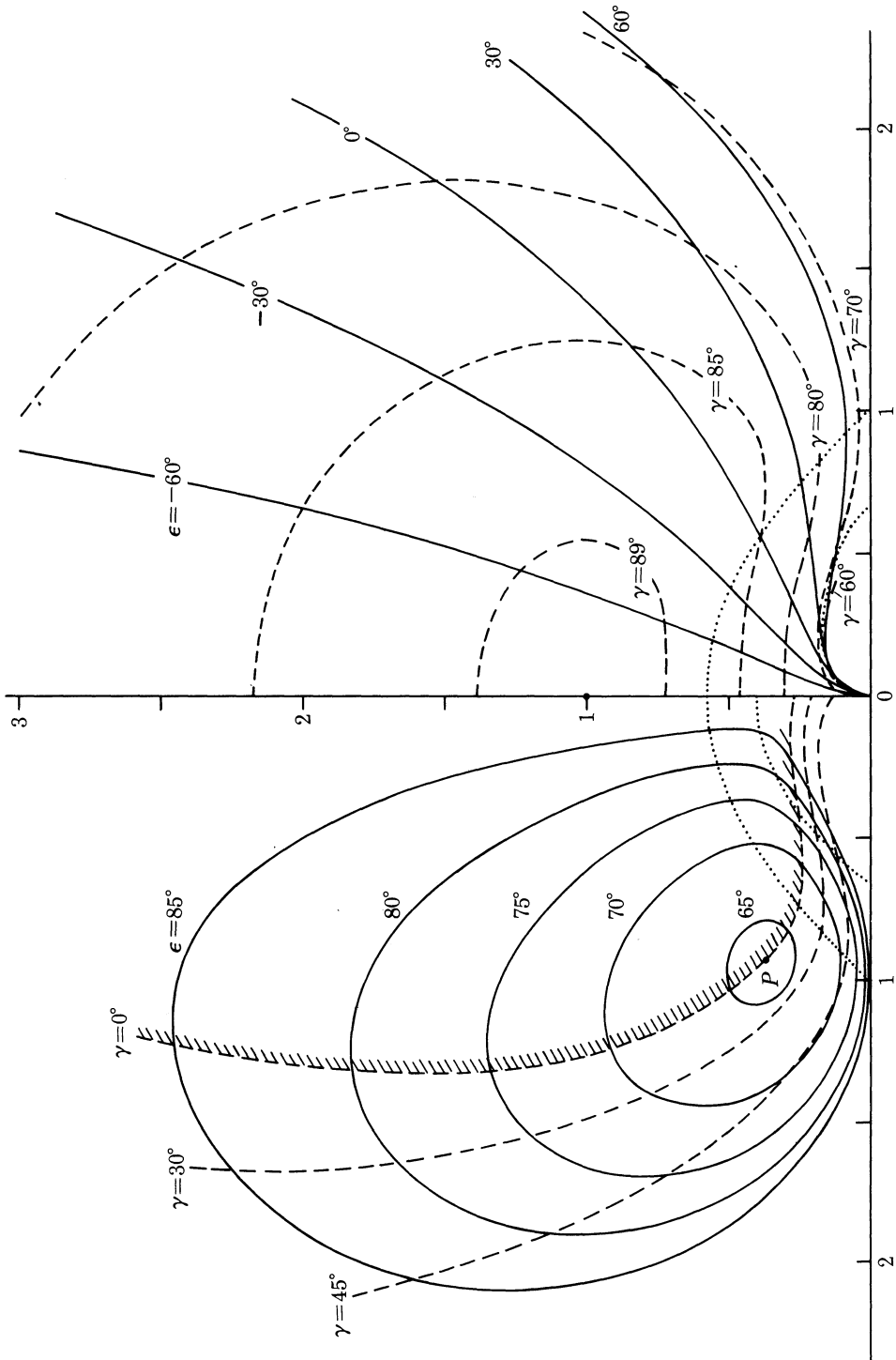


FIGURE 10. Loci of possible sharp corners at the free surface when  $U = 0$ , showing contours of  $\gamma$  and  $\epsilon$ . Dotted curves show points where  $Dp/Dt = 0$ .

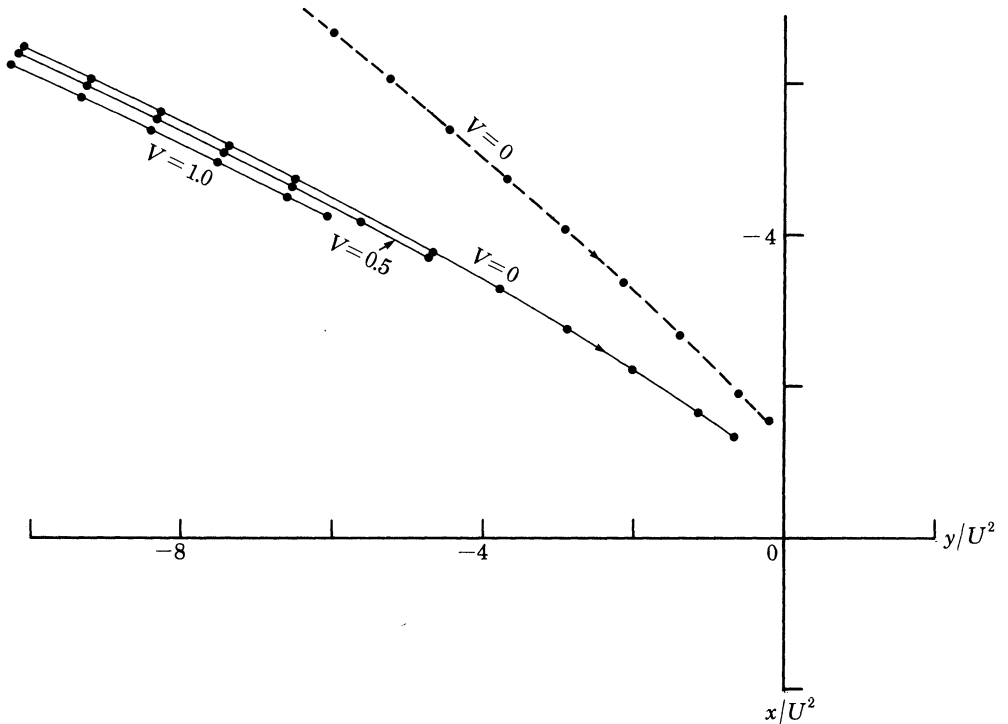


FIGURE 11. Loci of possible sharp corners at the free surface when  $U = -1$ . Solid curves show admissible solutions. Broken curve shows inadmissible solutions.

and to seek first solutions at large but finite values of  $r$  in the neighbourhoods of the two limiting solutions in figure 10. This was done, by starting with  $r = 10^6$  and solving (7.18) and (7.22) by iteration. The value of  $r$  was then gradually reduced, each solution being used as a starting point for the next.

Of the solutions obtained in this way, those starting from the inner of the two solution points in figure 10 corresponded to high values of  $\tilde{F}$  and were therefore unsuitable, by the criterion (6.19). Solutions starting from the outer point in figure 10 corresponded to smaller values of  $\tilde{F}$ . Some loci of possible cusps are shown in figure 11. The corresponding values of

$$f = \tilde{F} - \frac{1}{8}U - \frac{\sqrt{3}}{8}V$$

are generally not positive, as is required by equation (6.20). Nevertheless they can be made small enough to be acceptable.

An example is shown in figure 12, where we have  $f = -0.039$ , which is sufficiently small that the slight rise in level as  $t \rightarrow -\infty$  for large  $r$  may be accepted. The shape of the forward face, while concave as  $r \rightarrow \infty$ , is slightly convex at smaller values of  $r$ .

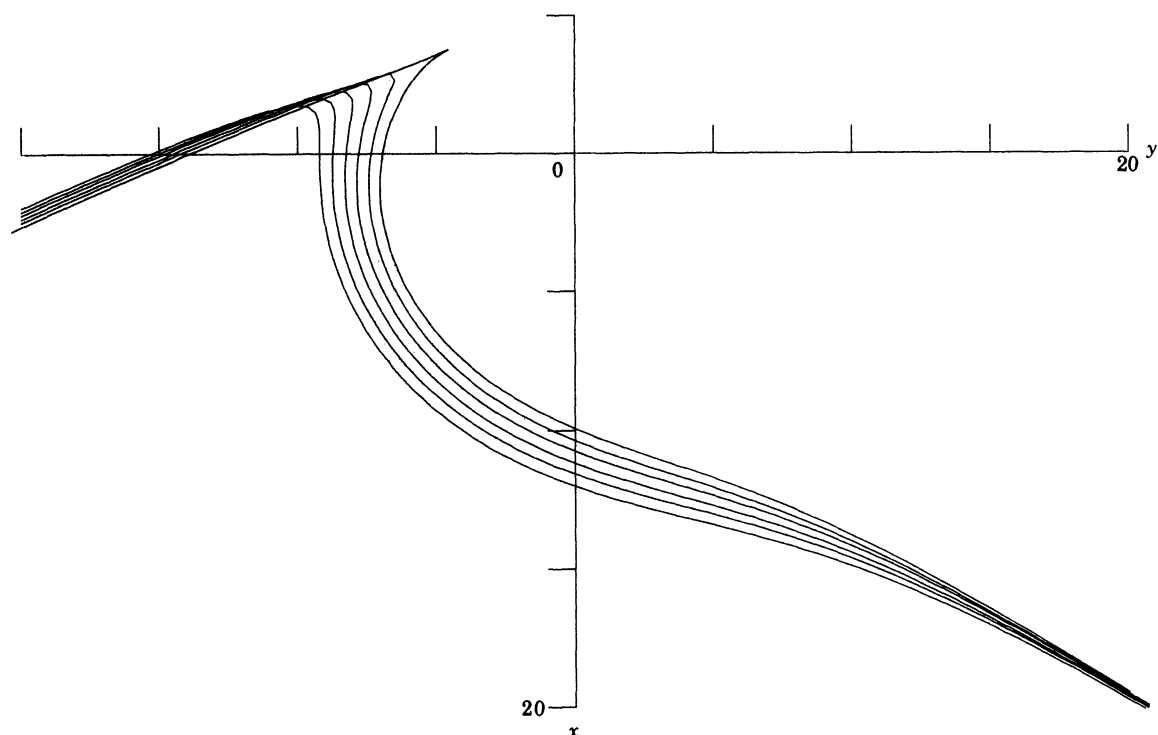


FIGURE 12. A time-sequence of surface profiles culminating in a cusp.  
 $U = -1$ ,  $V = 0$ ,  $\tau_c = 6.0$ .

### 8. DISCUSSION AND CONCLUSIONS

We have argued that, the flow in a breaking wave being multivalued, we must expect at least a branch-point in the velocity-potential  $\chi$ . The simplest possible branch-point is of order  $\frac{1}{2}$ , and we have shown that the three-term expression (6.1) is capable of describing, at least qualitatively, the most obvious features of plunging breakers, namely the overturning of the forward face and the apparent forming of a cusp at the tip.

It should be emphasized that the solutions are valid only approximately, and over a limited range of the time  $t$ . At the later stages of the flow it will be necessary to match the solution near the tip of the wave to a locally valid solution such as was described in Longuet-Higgins (1980*b*). The reason for our interest in the cusp-like solutions of § 7 is that these particular forms, with a small crest-angle, are most likely to be suitable for matching to the local flow.

Likewise, the earlier stages of the flow, when  $t$  is large and negative, must be matched to the flow in the rest of the wave, in a manner similar to that used for the almost-highest wave by Longuet-Higgins & Fox (1978), but the time-dependence also being included.

Thus we see the present solutions as essentially intermediate, in both space and time, between expressions describing the wave as a whole, which must take account of boundary conditions such as finite or decreasing depth of water, and the ultimate stage of breaking described locally as a jet or sharp corner.

The expression (6.1) may possibly be the first three terms of an asymptotically convergent series of decreasing powers of  $z^{\frac{1}{2}}$ . Further terms in the series could perhaps be determined in the same way in which we have determined  $A(t)$ . However, different forms would be required for non-progressive waves. For example, in a standing wave, with a vertical plane of symmetry, we should require a solution with at least two singularities, situated symmetrically on either side of the plane, or reflecting wall.

Naturally, any of the foregoing profiles may be viewed in a frame of reference moving with an arbitrary steady velocity  $U'$ , so that the branch-point appears to move in the opposite direction with speed  $-U'$ . Moreover we can obtain new solutions relative to axes with any acceleration  $\mathbf{a}$ , on replacing the gravitational acceleration  $\mathbf{g}$  by  $\mathbf{g}' = \mathbf{g} - \mathbf{a}$  and referring the new solutions to axes pointing in the direction of  $\mathbf{g}'$ .

#### APPENDIX. SHARP CORNERS: THE CASE $U = V = 0$

The following analysis provides starting values for obtaining solutions in the more general case.

When  $U = 0$ , equation (7.9) reduces to

$$\beta = -\tan \frac{1}{2}\theta \cos(\theta + \epsilon). \quad (\text{A } 1)$$

Since  $\beta$  has to satisfy (7.11), there is a critical point where

$$\partial\beta/\partial\theta = 0, \quad \beta = 1 \quad (\text{A } 2)$$

(hence  $a/r = 1$ ). Equations (A 1) and (A 2) lead immediately to

$$\cos\theta = \frac{1}{2}(1 - \sqrt{3}); \quad \theta = -111.47^\circ, \quad (\text{A } 3)$$

and

$$\epsilon = 64.41^\circ. \quad (\text{A } 4)$$

The loci of  $z/a = (r/a)e^{i\theta}$  are shown in figure 10. The critical point is designated by P. We show the quadrants  $-90^\circ > \theta > -180^\circ$  and  $-180^\circ > \theta > -270^\circ$ , the others being obtained by reflection in the origin.

In figure 10 the contours of  $\gamma$  are obtained from (7.17) by writing  $U = 0$ . However, the loci for  $Dp/Dt = 0$ , obtained from (7.22), simplify very considerably in this instance. For, since from § 6  $\dot{A}^* = -A$  and  $\dot{H} = -\frac{3}{2}iA$ , equation (7.22) implies that either

$$\dot{A} = 0 \quad (\text{A } 5)$$

or

$$\omega^{-1}(-i\omega^* + A^*/\omega^*) - \frac{3}{2}i - \text{c.c.} = 0. \quad (\text{A } 6)$$

Consider the first alternative (A 5). In that case  $\chi_t = 0$  and the motion must be steady (clearly an approximation). However, assuming this is so, we have from

(7.1) that

$$\chi_{zz}\chi_z^* = 1; \tag{A 7}$$

hence

$$\frac{1}{2}(i/\omega - A/\omega^3)(-i\omega^* + A^*/\omega^*) = 1, \tag{A 8}$$

that is

$$(i - B)(-i + B^*) = 2e^{i\theta}. \tag{A 9}$$

The real part gives

$$1 - BB^* = 2 \cos \theta. \tag{A 10}$$

But from (7.4) we have  $BB^* = a^2/r^2$ . Combining this with (A 10) gives

$$r/a = (1 - 2 \cos \theta)^{-\frac{1}{2}}. \tag{A 11}$$

This is the locus shown by the outer dotted lines in figure 9.

The second alternative (A 6) gives

$$i(\omega^2 - 3\omega\omega^* + \omega^{*2}) + (A - A^*) = 0, \tag{A 12}$$

that is

$$r(2 \cos \theta - 3) + 2a \sin \epsilon = 0. \tag{A 13}$$

Therefore

$$r/a = 2 \sin \epsilon / (3 - 2 \cos \theta). \tag{A 14}$$

This locus is represented in figure 9 by the two dotted arcs closest to the origin in each quadrant.

When the free surface corresponding to the above values is plotted as a function of time, however, it is found that the profiles have unphysical features; either they are strongly convex on their forward face, or else the limiting profiles with sharp corners are approached from the *outside*, as  $t$  increases, and not from the inside as desired. We have shown in § 7 that this difficulty is overcome by taking non-zero values of  $U$  and  $V$ .

This paper was begun in Cambridge and completed during a visit by the author to the Jet Propulsion Laboratory of the California Institute of Technology, Pasadena, between November 1979 and February 1980. For the hospitality and assistance given him there, he is much indebted to Dr O. H. Shemdin and Professor P. A. Saffman, and members of the Division of Earth and Space Sciences headed by Dr M. T. Chahine.

#### REFERENCES

- Longuet-Higgins, M. S. 1980*a* A technique for time-dependent, free-surface flows. *Proc. R. Soc. Lond. A* **371**, 441-451.  
 Longuet-Higgins, M. S. 1980*b* On the forming of sharp corners at a free surface. *Proc. R. Soc. Lond. A* **371**, 453-478.

- Longuet-Higgins, M. S. & Cokelet, E. D. 1976 The deformation of steep surface waves on water. I. A numerical method of computation. *Proc. R. Soc. Lond. A* **350**, 1–26.
- Longuet-Higgins, M. S. & Cokelet, E. D. 1978 The deformation of steep surface waves on water. II. Growth of normal-mode instabilities. *Proc. R. Soc. Lond. A* **364**, 1–28.
- Longuet-Higgins, M. S. & Fox, M. J. H. 1978 Theory of the almost-highest wave. Part 2. Matching and asymptotic expansion. *J. Fluid Mech.* **85**, 769–786.
- Price, R. K. 1971 The breaking of water waves. *J. geophys. Res.* **76**, 1576–1581.
- Stokes, Sir G. G. 1880 Supplement to a paper on the theory of oscillatory waves. *Mathematical and Physical Papers*, vol. 1, pp. 314–326. Cambridge University Press.